ISSN: 0974-5823 Vol. 7 No. 1 January, 2022

International Journal of Mechanical Engineering

Assessment of Fetal Health Detection and Diagnosis Using DCNN_LSTM Method

S. Fathimuthu Joharah
Research Scholar, Department of IT, Sri Ram Nallamani Yadava College of Arts & Science, Tenkasi, Tamilnadu, India,
Affliation of Manonmaniam Sundaranar University, Abishekapatti, Tirunelveli, Tamilnadu, India

Dr.S. Kother Mohideen
Assosciate Professor & Head, Department of IT, Sri Ram Nallamani Yadava College of Arts & Science, Tenkasi, Tamilnadu

***Abstract* - This paper suggests an architecture that allows for automated image_classification and captioning for better performance. In particular, the proposed approach implements a DCNN-LSTM (Deep Convolution Neural Network Long Short Term Memory Network) model that combines the global information and local information (hybrid features) extracted from given input image. This type of feature is firstly used to create local and global guiders, respectively. The whole captioning system consists of deep convolutional layers, these are separate into various distribution attributes prediction frame and branch feature extraction image. Two distribution information methods were used, are global and local inform for LSTM caption creation. We also implemented the methods to do dual caption and classification using DCNN-LSTM. The proposed DCNN-LSTM based capture model can reach efficient development over the state-of-the-art proposition.**

Keywords - DCNN_LSTM, Fetal images, Feature Extraction and performance, Filter.

INTRODUCTION

A new content-based image retrieval method in that texture and color feature used. In the color image two types of information is extracted such as color and texture feature, in which it is more accurate for image retrieval based upon their query request. By comparing to the conventional moments, the Zernike moments has less sensitive to noise in the descriptor for ideal region-based shape [1]. RGB image converted from the spot where his opponent's chromaticity space, the contents of the characteristics of the color of an image caught using distribution moments of Zernike chromaticity.

In recent times, research effort in the low-level visual features and high-level semantic gap is reducing between objects in the image. It discusses these aspects, the approaches used to extract low-level features. Color histograms, invariant color histograms, color moments, and dominant color system features are the color features extracted from Gabor Transform, Tamura features and the GLCM [2].

One of the unsupervised learning techniques is image clustering. For any particular problem cannot be separated on the basis of a novel multi-dimensional lifting schematic structure of the bandwidth filter bank discussed [3]. Content-based image retrieval system, the retrieval process of color, shape and texture features are used and which is mainly implemented in the medical industry, cosmetic industry and botanical gardening.

Lag value-based retrievals for reduce the texture spectrum in the medical images. According to the pathology bearer, the retrieval of the medical image is often processed so that the images are accurately separated and not automatically detected in the general case. Furthermore, low-level features such as color, texture, or shape are sufficient to describe medical images, not necessarily a high level of content understanding and interpretation of images, indicating their automatic segmentation as a result of medical images. Such systems require high level of query completion and accuracy to make them reliable from a clinical point of view [4].

Thus Content-based image retrieval system retrieves the image based on color, shape and texture features by bridging low-level visual features and high-level semantic gap. These systems are gaining importance in medical industry as it helps to retrieve the relevant image.

The organization of this paper work as follow: In section 1 implicates the introduction, in section 2 shows the study of different research work along with our system. The next section explains the proposed system and deep convolutional neural network and long short-term memory algorithms and steps. In section 4 represent the result and discussion, it shows the fetal image outputs along with performance measures. Finally, section 5 shows the conclusion part.

LITERATURE SURVEY

The user's interest is retrieving a content-based image is part of the image. The first desired object identification with the rest of the image is accordingly not related to the weight that it is labeled in combination with a multi-instance learning algorithm. It is used to sequence informational images using the similarity measure that is based on the parts of the image [5]. Auto reduction of a key points using segmentation that maintains the diversity required of image retrieval translated to the number of limit key points in each area received. Haar wavelet-based detection method is used in a critical point and divides the window into the neighbor's representation. The window is known to separate the individual object can be best captured in color and texture. Due to the nature of the gradient descent K-means, a widely used algorithm can be set as a partition, it is very sensitive to the initial cluster center. The number of iterations of the first iteration of the K-means is less than one initialization followed by the squared error sum between the two iterators to a maximum of 100, the second being a relative improvement, the second being controlled in both ways [6].

Thus segmentation-based and key point-based techniques were used for comparison but however the accuracy level remained low.

Templates feature extraction from a statistical approach used in space and time. The use of icon space transformation and canonical space transformation for feature extraction. Eigen space transformation and canonical space transformation from spatial templates and temporal templates into integrating feature vectors into an extended feature [7]. The spatial information is included in each spatial template and the movement between the two consecutive spatial templates is the symbol of the global template for both spatial information. The accreditation program is based on low-level features, and does not require detection or monitoring of object-specific areas. This method of data dimensionality reduction and simultaneously displays different style can be employed to improve class reparability.

A new multi-scale statistical modeling-based image of a new coherence function with two novel vectors based on a novel Kullback exclusion approach for features that make good conceptual refreshments, and less complex predictions [8]. The image system consists of a class of wavelet domain and statistical models including a Gaussian mixture model, as well as a generalized Gaussian mixture model employed to extract the wavelet domain features. This method outperforms most other conventional methods of recovery performance at a comparable level of complexity predictions.

Training and classification are the two modes of recognition system. In training mode, feature extraction selection module features input formats suitable for representing the division of space to practice finding and classifying feature. In the classification system, training the classifier on the basis of the measured features of the classes under consideration corresponds to the input pattern [9]. The extraction process should improve on the feature proposed with respect to the recovery of the near-regression-based efficient repetitive processing system. Convolution Neural Network regression basis a repeatable procedure this time to retrieve the system image to improve the statistics feature extraction efficiency [11]. The variance decreases when the regression is performed at the CNN. The use of regression at CNN significantly improves retrieval rates, especially for large values of K.

Images classified by the same texture will be updated in order to be closer to the respective vectors as feature vectors [10]. Assessing different system recovery technologies, this method has been proven to provide significant improvement at a lower computational cost. An image representation method is presented using color correlation vector quantization (VQ). There are five textural features in the HSV, the three-color features of the color model, and the gray matrix co-occurring matrix. Once an image is retrieved, the eight-dimensional feature vectors represent each pixel in the image. Benign and malignant genetic algorithm-based feature selection method classifies a micro calcification cluster. Image Retrieval Features discusses the similarity between the set of query image features and how the information should be calculated using the image similarity measure.

METHODOLOGY

Our first model consists of a one layered LSTM that is used for both segmentation and feature extraction. It generates a combined multimodal fixed approach to focus on frame attribute extracted by DCNN method and word quality encoded by a long short term memory system shown in figure.1. When applying segmentation in this technique, it will convert from frame model to visualize text by content structure neural language method [14].

This design puts the responsibility of both input features and the natural language description in one set of weights which complicates the convergence of the network. This method used to recognize deep layer of frame and generate a text of captured images. DCNN is a common for frame observation and it illustrates a scripted digital identification with a back-propagation system.

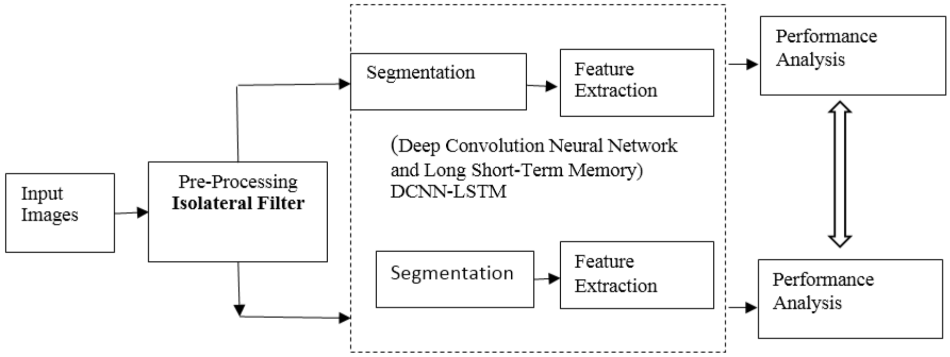

FIGURE 1
PROPOSED SYSTEM FLOW DIAGRAM FOR THE FETAL SEGMENTATION

The initial step of the proposed novel technique is to preprocess the fetal image hinge on the **Isolateral filtering (IF)**method. While preprocessing, an input ultrasound image undergoes noise eradication engendered during image generation which in turn eliminates the undesirable signals which can entail certain errors in the course of processing. The fetal images are mostly nobbled by certain noise which integrates Gaussian noise, visual noise and speckle noise.

Algorithm: Isolateral Filter

Step 1: Convert input image to double.
Step 2: Initially calculate the Gaussian distribution function.
Step 3: Initialize the weight of the Gaussian distribution.
Step 4: Calculate Euclidean distance of each pixel value.
The new pixel level value (k) is calculated for each of the brightness values in the original image, as given in Equation (1),

$$k = \sum_{i=0}^{j} N_i / T \qquad (1)$$

Where the sum calculates the number of pixels by determining the integration of the histogram with brightness less than term *j* and T is the total pixel value.
Step 5: Calculate the finite difference after which distribution function is evaluated.

Proposed Deep Convolution Neural Network and long short-term memory (DCNN-LSTM) algorithm

In order to avoid the situation corresponding to the features a new DCNN-LSTM segmentation approach for color imaging segmentation is proposed which overcomes the existing limitations. The proposed DCNN-LSTM algorithm is mentioned below.

Input: A fetal image; numbers of C; m=3; Threshold ε; maximal number of iterations>0

Output: Segmented image,

The algorithm for proposed segmentation Deep Convolution Neural Network and long short-term memory (DCNN-LSTM) algorithm is given below:

Step 1: Assign loop counter t=0.
Step 2: Determine the objective function of equation (3.1) for the given digital fetal image.
Step 3: Extract the fetal features for the input image and find the objective using equation (9) and represent it as C_2.
Step 4: Determine the objective function of DCNN-LSTM for the input digital fetal represented as (C_{add}).

$$C_{add}(v,u) = 2\left[\begin{array}{l} \sum_{i=1}^{N}\sum_{j=1}^{C}\mu_{ij}^{m}(1-k(xi,vj)) \\ +\sum_{i=1}^{N}\sum_{j=1}^{C} ri\,\mu_{ij}^{m}(1-k(\overline{xi},vj)) \end{array}\right] \qquad (3.1)$$

Step 5: Calculate C by using equation

$$C = C_1+C_2+C_{add} \rightarrow \min \qquad (3.2)$$

Where C_1 is the Objective function of from step1.
C_2 represents the fetal feature information obtained from step2.
$C_{add}$is the objective function of Adaptive Regularized Kernel based on the algorithm.

Step6: $C = \sum_{k=1}^{N}\sum_{j=1}^{C}\mu_{kj}^{m}\left\|X_k - V_j\right\|^2 + \sum_{k=1}^{N}\sum_{j=1}^{C}\mu_{kj}^{m}R_{jk}^{2} + \sum_{k=1}^{N}\sum_{j=1}^{C}\mu_{kj}^{m}\left(\frac{1}{1}\sum_{1=1}^{1} w_{ik}\right) + 2\left[\sum_{i=1}^{N}\sum_{j=1}^{C}\mu_{ij}^{m}(1-k(xi,vj))\right] +$

$$\left[\sum_{i=1}^{N}\sum_{j=1}^{C} ri\mu_{ij}^{m}(1-k(\overline{xi},vj))\right] \to \min \sum_{j=1}^{C}\mu_{kj}=1;\ \mu_{kj}\in[0,1]; \tag{3.3}$$

Step 7: Find the Centre of the cluster by taking derivative of C and equate to zero.

Step8: Calculate $V_j = \frac{\sum_{k=1}^{N}(\mu_{kj}^{m} + \left|\mu_{kj} - \overline{\mu_{kj}}\right| X_k}{\sum_{k=1}^{N}(\mu_{kj}^{m} + \left|\mu_{kj} - \overline{\mu_{kj}}\right|}$ (3.4)

Step 9: Find the membership matrix by using the formula

$$\mu_{kj} = \frac{-\lambda_k + 2\overline{\mu_{kj}}\left\|X_k - V_j\right\|^2}{2*(2\left\|X_k - V_j\right\|^2 + R_{jk}^2 + \frac{1}{1}\sum_{i=1}^{1} w_{ik})} \tag{3.5}$$

$$\lambda_k = \frac{\left(\sum_{j=1}^{C}\frac{\overline{\mu_{kj}}\left\|X_k - V_j\right\|^2}{(2*\left\|X_k - V_j\right\|^2 + R_{jk}^2 + \frac{1}{1}\sum_{i=1}^{1} w_{ik})} - 1\right)}{\left(\sum_{j=1}^{c}\frac{1}{2(2*\left\|X_k - V_j\right\|^2 + R_{jk}^2 + \frac{1}{1}\sum_{i=1}^{1} w_{ik})}\right)} \tag{3.6}$$

If t > 100 stop. Otherwise update t=t+1 and go to step 2.

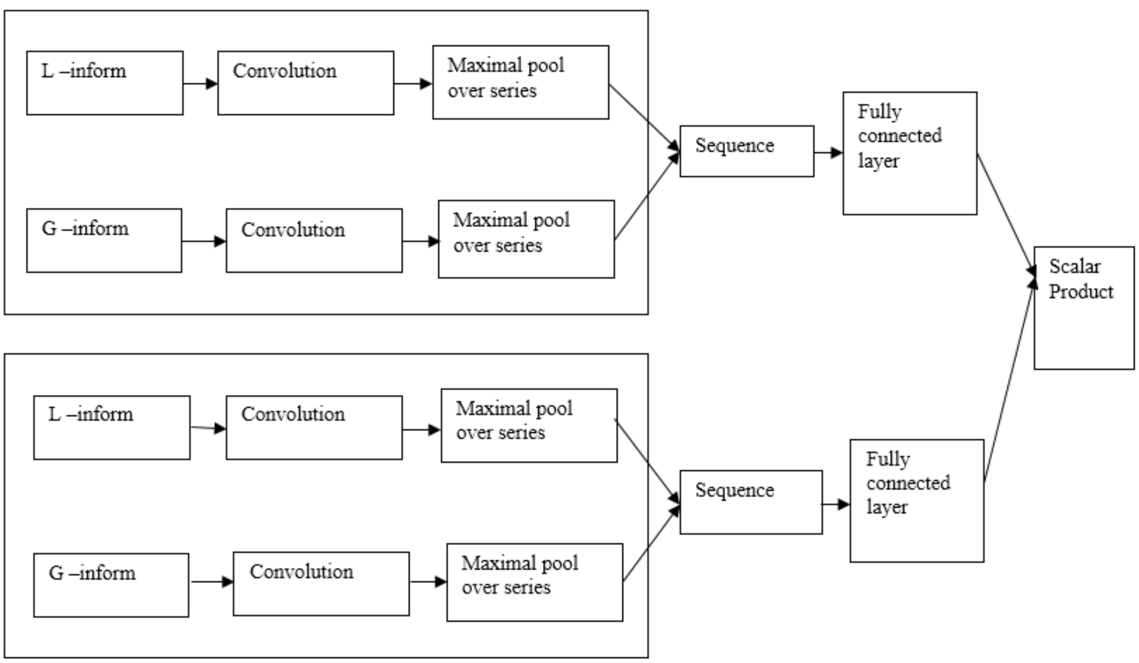

FIGURE 2

SCALAR PRODUCT OF TOP LOCAL- GLOBAL INFORMATION AND BOTTOM LOCAL-GLOBAL INFORMATION

Global and Local Information

In this section, we declare our double information related method. The scalar product of learning inactive representations from evaluation text. When we use similar system structure for item network and user. So, in detail we can explain about user system: the top block is local information related method (L-inform) this observe from local information keyword. The bottom block is the global information related method (G-inform) this observe from real review text series. This global inform and local inform were combined and send to fully-connected layers (FC) from the prepared portrayal of client category forecast. This mean italic lower occurrence from scalar (x, y), lower occurrence from vector (x, z), and the large dimensional variable grids with powerful upper occurrence (X, W). Likewise, MATLAB is used for cluster ordering, therefore, w (i, j) implies components of j[th] segment of the framework W.

1. Local and global attribute extraction: Obtaining dual attribute as input frame using DCNN.
2. Local-global information: Combining local attribute with global attribute through consideration system.
3. Frame description creation: Creating a sentence to declare the text of an input frame with LSTM term.

Embedding Layer

The text we use in fixed later for input frame document D_u, a pair of reviews from client u. This model of layer will be create as an improved performance that observe from single point vector, $\boldsymbol{e_t} \in \boldsymbol{R}^{|\boldsymbol{v}|}$, the input from a text is embedded in to heavy radius vector, $x_t = (x_1, x_2, \ldots, x_d)$ and $\boldsymbol{x_t} \in \boldsymbol{R^d}$, When fixed layer load is $w_e \in R^{d \times |v|}$

$$x_t = w_e e_t \tag{3.7}$$

V is text pair and |V| is area of lexicon.

Local Information (L-inform) Left Module

From this method, a local information constituent will Illuminate-L and used to utilize a word of window, which gradually increase by text. The embedded text from distance T were written by D_u (x_1, x_2,x_t). At that point, we apply the consideration through sliding parts to this succession. The center text has a chance from X_i and w is reconstructed width. The parameter lattice has processed with score weighting for every single text in predisposition as pursues

$$\begin{aligned} s(i) &= g(X_{l-\inf orm}, \\ & i * W^1_{l-\inf orm} + b^1_{l-\inf orm}), \qquad i \in [1, T]. \end{aligned} \tag{3.8}$$

Where L is an activity which implies component astute augmentation and aggregate. We utilize the sigmoid capacity (σ) for the initiation work, g(.) The score was considering as S(i), which used to utilize an embed text of ith consequence. Another text from given value has few attain in decipher, it generates small amount of text value in low significant then large amount of value in this method

$$\hat{X}^L_t = s(t) X_t \tag{3.9}$$

$\hat{\boldsymbol{X}}^{\boldsymbol{L}}_{\boldsymbol{t}}$ ***where*** $\boldsymbol{t \notin [1, T]}$ have heavy load series from text embedding's. The heavy load series from text embedding are send across convolutional layered with the help of kernel area of one (1x1) convolution were introduced first. Most kernel length are bigger than one should be used for this method. When the local information is generated to get single preference or attribute keywords for client/module, the kernel length one was fixed exactly for this purpose, for fitting its effected lowly.

The fixed size condensed vector was extracted for maximal pooling over the series. It results, local information description from given word to be obtaining as follows by scalar matrix convolution $W^2_{l-\inf orm} \in R^{d \times n_{l-\inf orm}}$ *and a bias* $b^2_{l-\inf orm} \in R^{n_{l-\inf orm}}$ and max pooling:

$$Z_{l-\inf orm}(t, i) = g(\hat{x}^L_t * W^2_{l-\inf orm}(:, i) + b^2_{l-\inf orm}(i)), \tag{3.10}$$
$$i \in [1, n_{l-\inf orm}]$$

$$Z_{l-\inf orm}(i) = Max(Z_{l-\inf orm}(:, i)). \tag{3.11}$$

Number of layers are representing as $n_{l-\inf orm}$ and tanh parameter represent g(.)

Global Information (G-inform) Right Module

The series of text from $D_u$is an input text from global information method, G-inform. The input module sends through G-inform layer by increasing the G-inform method scores by self. This execution is related to that L-inform, and the whole input word computed the information scores. Let $\hat{X}^G_t$ be a heavy load to embedding text of G-inform method where $\boldsymbol{t \in [1 : T]}$. When general information surface is used for uninformative texts effects are deployed from global feature meaning is took with precise from the declared CNN layer. When we fixing the size of filter as w_f, it means the filtered layer operates from w_f texts in convolutional layer. When the number of layered filters is $n_{g-\inf orm}$, the filter convolution is $W_{g-\inf orm} \in R^{w_f \times d \times n_{g-\inf orm}}$ are applied to a series of w_f load text embedding's, $\hat{X}_{g-\inf orm,i} \in R^{w_{f\times d}}$, and the output attribute $Z_{g-\inf orm} \in R^{(T-w_f+1)\times n_{g-\inf orm}}$:

$\hat{X}_{g-\inf orm}, i = (\hat{x}_i^G, \hat{x}_{i+1}^G, ...\hat{x}_{i+w_{f-1}}^G)^T$, (3.12)

G(.) is a tanh consequence and $b_{g\text{-inform}}$ is a vector bias. The maximal pool over a series were selected by heuristically pooled layer $z_{g-\inf orm}(j) = Max(Z_{g-\inf orm}(:, j))$. The applied $z_{g\text{-inform}}$ as the number of various filter size w_f. In this process, n_w various filter size are used as follows.

Terminal Layers

The outputs of the global and local information n method are combined, and execute through further fully connected layers W_{FC}^1 *and* W_{FC}^2 :

$$z_{out}^1 = z_{l-\inf orm} \oplus z_{g-\inf orm}^1 \oplus ....\oplus z_{g-\inf orm}^{n_w}, \quad (3.13)$$

$$z_{out}^2 = g(W_{FC}^1.z_{out}^1 + b_{FC}^1), \quad (3.14)$$

$$\gamma_u = g(W_{FC}^2.z_{out}^2 + b_{FC}^2). \quad (3.15)$$

$\oplus$ is a combined operator.g(.) is a tanh parameter.

Global and Local Features Extraction

The local information and global information are major for representing a frame. It highlights generally contain the setting data around articles, and neighborhood includes dependably contain the fine-grained data of items. Along these lines, in this paper, we investigate the two major portraying the substance of a picture. Profiting by the amazing portrayal of CNNs, picture characterization and item identification have gained extraordinary ground. In this paper, we remove worldwide element and neighborhood highlights with Faster DCNN. We separate worldwide component from fc7 layer of VGG16 net, a 4096-measurement vector indicated as Gf. The VGG16 net is prepared on Image Net grouping dataset. For neighborhood highlights meant as {Lf1, ..., Lfn}, we select top-n recognized articles to speak to significant nearby items as indicated by their group certainty scores acquired from DCNN. At that point, we speak to each item as a 4096-measurement CNN highlight vector separated from fc7 layer for each article jumping box. Along these lines, each picture can be at long last spoken to as a lot of 4096-measurement vectors I={Gf,Lf1,...,Lfn}. In our tests, we set n to 10 since the quantity of item contained in a picture is as a rule beneath 10.

Global-local Information Mechanism

The local information with global information is major model for describing frame. In our proposed model, we assume recognition mechanism to synthesize those two models of information according to the subsequent Eq. 3.16:

$$\Psi^{(t)}(I) = \alpha_0^{(t)} Gf + \sum_{i=1}^{n} \alpha_i^{(t)} Lf_i, \quad (3.16)$$

Where $\alpha_i^{(t)}$ represent the information load of separate attribute at time t and $\sum_{i=0}^{n} \alpha^{(t)} = 1$.

This component progressively loads each element by allocating it with one positive weight αi(t) alongside the sentence age method. Through this way, our strategy can specifically concentrate on some striking articles at various time and consider their setting data in the meantime. The consideration weight αi(t) measures the significance level of each component at time t and the pertinence of each element to the past data. Subsequently, it very well may be registered dependent on the past data and each element fi $\in \{Gf, Lf_0, ..., Lf_n\}$ with the accompanying conditions:

The information heavy load is obtained by standardize with softmax reversion. H(t-1) is the past concealed state yield which will be presented in the following segment. W, W_h, W_o *and* b are the parameters to be learned by our model and shared by every one of the highlights at all the time steps. Φ is initiation work.

RESULT AND DISCUSSION

Figure 3. Segmentation results obtained from different deep learning architectures. For the two boxes, from left to right (columns): uterus, lungs, brain, umbilical cord, and placenta in MRI and US. From top to bottom (left box—rows): (1) ground truth (the sub-box highlighted in blue), (2) U-Net, (3) V-Net,

TABLE 1
PERFORMANCE METRICS FOR FEATURE EXTRACTION

Feature (Type)	Alone	W/O

	PRCS	RECALL	DC	PRCS	RECALL	DC
Dependence Non-uniformity (GLDM)	0.33∓0.46	0.32 ∓0.32	0.27 ∓0.39	0.89 ∓0.05	0.76 ∓0.06	0.82 ∓0.05
Mean Absolute Deviation (First Order)	0.91∓ .04	0.7∓ 0.07	0.76∓ 0.05	0.90 ∓0.04	0.76 ∓0.10	0.80 ∓0.07
Inverse Difference Normalized (GLCM)	0.87 ∓0.04	0.74∓ 0.10	0.76∓0.05	0.90 ∓0.05	0.71 ∓0.06	0.78 ∓0.04
Long Run Emphasis (GLRLM)	0.92 ∓0.06	0.74∓ 0.10	0.76 ∓0.05	0.90 ∓0.05	0.71 ∓0.06	0.78 ∓0.04
Uniformity	0.90∓ 0.04	0.55 ∓0.25	0.60 ∓0.28	0.90∓ 0.02	0.72 ∓0.06	0.78 ∓0.05
Contrast (GLCM)	0.93∓0.01	0.66∓ 0.11	0.75 ∓0.08	0.93 ∓0.01	0.74 ∓0.10	0.80 ∓0.07

For execution assessment, parameters of the proposed classification proposal such as characterization of specificity, sensitivity and accuracy of proposed method are calculated. The performance measures are as follows:-

Accuracy = (TP/TN)/ (TP+TN+FP+FN)*100%

Specificity =TN/ (TN+FP)*100%

Sensitivity =TP/ (TP+FN)*100% where

True positive (TP): Reported as fetal as well as biopsy.

True negative (TN): Not reported as fetal as well as biopsy.

False positive (FN): Reported as fetal but not on biopsy.

False negative (FN): Not reported as fetal but reported on biopsy.

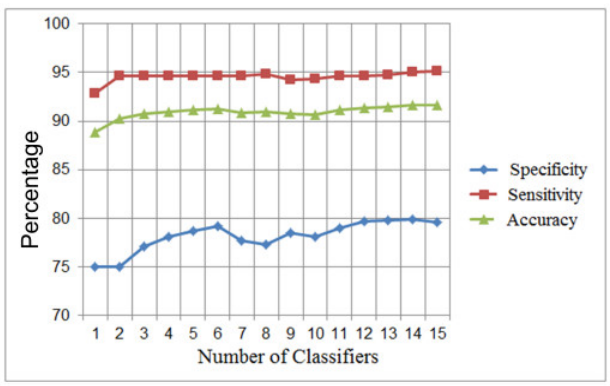

FIGURE 4
PERFORMANCE GRAPH OF CLASSIFIER

TABLE 2
COMPARISONS OF CLASSIFIER ACCURACY AND ERROR VALUES

Classifier	KNN	SVM	CNN [12]	DCNN-LSTM [13]
Accuracy (%)	86.7	90	92	97.3
Error (%)	13.3	10	8	2.8333

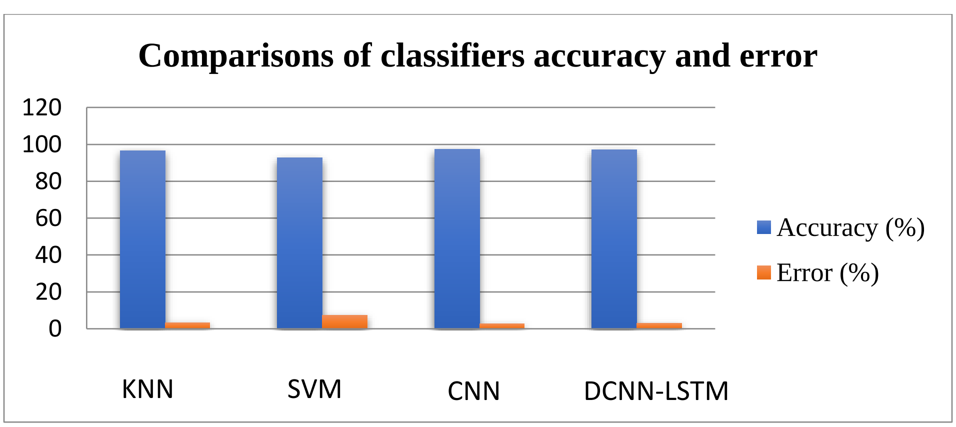

FIGURE 5
CLASSIFIER'S ACCURACY AND ERROR COMPARISONS

From the comparison figure 5 the accuracy is high for KNN and SVM classifiers. DCNN-LSTM classifier accuracy will be 97.3%. If the error is high, then the accuracy will be low.

TABLE 3
DCNN-LSTM CLASSIFIER STANDARD METRICS VALUES OF IN VARIOUS FEATURE COMBINATION

Features	Sensitivity	specificity	accuracy	precision	similarity	border error
HOG	90	96	92.7	96.4	92.5	7.3
GLCM	91.3	79	85.4	81	86.5	14.6
FOS	91.3	79	85.4	81	86.5	14.6
HOG+GLCM	91.3	79	85.4	81	86.5	14.6
Gabor+FOS	80.5	67	74	71.6	75.5	26
GLCM+FOS	85	71.5	78	75	80	22

Table 3 shows that the standard metrics values of various features, these are output from the CNN classifiers. From the table, we can understand which feature combinations gives the higher accuracy of the classifiers. Border error denotes how many skin images are represented wrongly. HOG gives the higher accuracy of 92.7%. GLCM, FOS, and HOG + GLCM give the accuracy of 85.4%. Gabor + FOS and GLCM + FOS give the worst accuracy.

CONCLUSION

Early fetal image detection and treatment response evaluation present major challenges in the radiological work-up of patients at risk and patients who have already developed fetal. Intensified screening programs with state-of-the-art imaging techniques and advanced image post-processing algorithms are being developed and hold the potential to improve patient outcome. In this paper, the neural network is used in feature extraction and classification. By using the neural network, the accuracy performance provided better to comparing other machine learning techniques.

The following explorations can be made by researches in future:

- In this system, only three features are considered as feature vector for image representation. Equal weightage is given to all the three features. In additional to this, more low-level image descriptors (e.g, color, texture, shape etc.,) may be considered as feature vector for image representation. Based on the property of features, due weightage may be given.
- Other neural techniques may be considered to measure the segmentation and classification in fetal images. In addition to this, comparing other algorithms may be considered to increase the performance.

REFERENCES

[1] Torrents-Barrena, J., López-Velazco, R., Piella, G., Masoller, N., Valenzuela-Alcaraz, B., Gratacós, E., & Ballester, M.Á.G. (2019). TTTS-GPS: Patient-specific preoperative planning and simulation platform for twin-to-twin transfusion syndrome fetal surgery. *Computer methods and programs in biomedicine, 179*, 104993.

[2] Calderon, S., Fallas, F., Zumbado, M., Tyrrell, P.N., Stark, H., Emersic, Z., & Solis, M. (2018). Assessing the impact of the deceived non local means filter as a preprocessing stage in a convolutional neural network based approach for age estimation using digital hand x-ray images. *In 25th IEEE International Conference on Image Processing (ICIP)*, 1752-1756.

[3] Benoist, G., Salomon, L.J., Mohlo, M., Suarez, B., Jacquemard, F., & Ville, Y. (2008). Cytomegalovirus-related fetal brain lesions: comparison between targeted ultrasound examination and magnetic resonance imaging. *Ultrasound in Obstetrics and Gynecology: The Official Journal of the International Society of Ultrasound in Obstetrics and Gynecology, 32*(7), 900-905.

[4] Henderson, J., Kesmodel, U., & Gray, R. (2007). Systematic review of the fetal effects of prenatal binge-drinking. *Journal of Epidemiology & Community Health, 61*(12), 1069-1073.

[5] Kajantie, E. (2006). Fetal origins of stress-related adult disease. *Annals of the New York Academy of Sciences, 1083*(1), 11-27.

[6] Monk, C., Feng, T., Lee, S., Krupska, I., Champagne, F.A., & Tycko, B. (2016). Distress during pregnancy: epigenetic regulation of placenta glucocorticoid-related genes and fetal neurobehavior. *American Journal of Psychiatry, 173*(7), 705-713.

[7] Lebel, C., Rasmussen, C., Wyper, K., Andrew, G., & Beaulieu, C. (2010). Brain microstructure is related to math ability in children with fetal alcohol spectrum disorder. *Alcoholism: Clinical and experimental research, 34*(2), 354-363.

[8] Georgieva, A., Papageorghiou, A.T., Payne, S.J., Moulden, M., & Redman, C.W.G. (2014). Phase-rectified signal averaging for intrapartum electronic fetal heart rate monitoring is related to acidaemia at birth. *BJOG: An International Journal of Obstetrics & Gynaecology, 121*(7), 889-894.

[9] Kvarnstrand, L., Milsom, I.A.N., Lekander, T., Druid, H., & Jacobsson, B.O. (2008). Maternal fatalities, fetal and neonatal deaths related to motor vehicle crashes during pregnancy: A national population-based study. *Acta obstetricia et gynecologica Scandinavica, 87*(9), 946-952.

[10] Ebner, M., Wang, G., Li, W., Aertsen, M., Patel, P.A., Aughwane, R., & Vercauteren, T. (2020). An automated framework for localization, segmentation and super-resolution reconstruction of fetal brain MRI. *NeuroImage, 206*, 116324.

[11] Rundo, L., Han, C., Nagano, Y., Zhang, J., Hataya, R., Militello, C., & Cazzaniga, P. (2019). USE-Net: Incorporating Squeeze-and-Excitation blocks into U-Net for prostate zonal segmentation of multi-institutional MRI datasets. *Neurocomputing, 365,* 31-43.

[12] Islam, M.Z., Islam, M.M., & Asraf, A. (2020). A combined deep CNN-LSTM network for the detection of novel coronavirus (COVID-19) using X-ray images. *Informatics in medicine unlocked, 20,* 100412.

[13] Tian, Y., & Fu, S. (2020). A descriptive framework for the field of deep learning applications in medical images. *Knowledge-Based Systems, 210,* 106445.

[14] Liu, S., Wang, Y., Yang, X., Lei, B., Liu, L., Li, S.X., & Wang, T. (2019). Deep learning in medical ultrasound analysis: a review. *Engineering*, *5*(2), 261-275.

[15] Rotem-Kohavi, N., Williams, L.J., & Oberlander, T.F. (2020). Advanced neuroimaging: a window into the neural correlates of fetal programming related to prenatal exposure to maternal depression and SSRIs. *In Seminars in perinatology, 44*(3), 151223.